ELSEVIER

Journal of Alloys and Compounds 330–332 (2002) 702–707

Journal of ALLOYS AND COMPOUNDS

www.elsevier.com/locate/jallcom

Microstructural characterization of catalyzed $NaAlH_4$

G.J. Thomas[a,*], K.J. Gross[a], N.Y.C. Yang[a], C. Jensen[b]

[a]*Sandia National Laboratories, Livermore, CA 94550, USA*

[b]*University of Hawaii, Chemistry Department, Honolulu, HI 96822, USA*

Abstract

A number of laboratories have now demonstrated that catalyst-assisted $NaAlH_4$ can reversibly absorb and desorb hydrogen in the solid state at moderate temperatures. An understanding of the mechanisms by which bulk decomposition and reformation of the compound can occur in the presence of a surface catalyst is important to improving the kinetic and thermodynamic properties of alanates for use in hydrogen storage applications. Using scanning electron microscopy (SEM) and energy dispersive spectroscopy (EDS), we have examined the microstructure and elemental composition of Na alanate samples, doped using a liquid Ti/Zr catalyst precursor, for a number of conditions. First, microscopy and compositional analyses were performed at different stages of the decomposition process within the first desorption cycle. Second, the material was characterized after multiple absorption/desorption cycles (five cycles). Finally, the effects of the catalyst doping procedure on particle size, surface morphology and surface composition were examined. Significant changes in particle morphology and in elemental distribution were found to be induced by the desorption and cycling processes. Importantly, our measurements indicate that the initial dehydriding reactions were accompanied by significant enhancement of Al concentration toward the surface of particles and that elemental segregation occurred with repeated absorption/desorption cycles.

Keywords: Metal hydride; Complex hydride; Hydrogen storage; $NaAlH_4$; Na_3AlH_6; Electron microscopy

1. Introduction

The results of Bogdanovic and Schwickardi [1], which showed reversible hydriding behavior in the Ti-doped alanate hydrides $NaAlH_4$, Na_3AlH_6 and Na_2LiAlH_6, has spurred renewed interest in the use of alanates as hydrogen storage materials. Unlike intermetallic hydrides, these complex-based hydrides release hydrogen through a series of decomposition reactions as described in the following two equations:

$$NaAlH_4 \leftrightarrow \tfrac{1}{3}Na_3AlH_6 + \tfrac{2}{3}Al + H_2 \quad (1)$$

$$Na_3AlH_6 \leftrightarrow 3NaH + Al + \tfrac{3}{2}H_2 \quad (2)$$

Thus, $NaAlH_4$ first decomposes to evolve molecular hydrogen and form an intermediate compound, Na_3AlH_6, and metallic Al. This intermediate phase then decomposes to NaH with additional metallic Al formation and hydrogen evolution. It is somewhat surprising that these reactions can occur reversibly in the solid state and at the low temperatures which have been reported in the literature [1–4]. Furthermore, in-situ X-ray diffraction studies by Gross et al. [3] indicate the formation of relatively large crystallites of Al during decomposition reactions, suggesting long range transport of metallic species. What then are the processes by which the reactions in Eq. (1) can take place nearly to completion? How can a surface catalyst affect reactions occurring within the bulk of solid particles? Clearly, an understanding of the solid state mechanisms by which bulk decomposition and reformation of the compounds occur in the presence of surface catalysts is important to improving the kinetic and thermodynamic properties of alanates for use in hydrogen storage applications.

Using scanning electron microscopy (SEM) and energy dispersive spectroscopy (EDS), we have examined the microstructure and elemental composition of Na alanate samples doped using a liquid Ti/Zr catalyst precursor [2]. This material was observed for a number of conditions. First of all, microscopy and compositional analyses were performed at different stages of the decomposition process within the first desorption cycle; that is, fully hydrided $NaAlH_4$, partially dehydrided to the Na_3AlH_6 composition

*Corresponding author. 537 Spirit Ridge Court, Reno, NV 89511, USA. Tel.: +1-775-851-2702; fax: +1-775-851-2780.

E-mail address: gjthomas1@earthlink.net (G.J. Thomas).

0925-8388/02/$ – see front matter
PII: S0925-8388(01)01538-9

and fully dehydrided material to the NaH phase. Since the initial state of the material is fully hydrided, the first cycle consists only of a desorption step. Further, the material was characterized after multiple absorption/desorption cycles (five cycles). Finally, the effects of the catalyst doping procedure on particle size, surface morphology and surface composition were examined. Significant changes in particle morphology and in elemental distribution were found to be induced by the desorption and cycling processes. Importantly, our measurements indicate that the initial dehydriding reactions were accompanied by significant enhancement of Al concentration toward the surface of particles and that elemental segregation occurred with repeated absorption/desorption cycles. These results are consistent with the observation of metallic Al by in-situ X-ray diffraction experiments during hydrogen evolution from catalyzed alanates [3].

2. Experimental procedures

2.1. Microscopy

Na alanate is very sensitive to air and water exposure, reacting strongly with O_2 and OH. Hence, all material processing was performed in a dry Ar glovebox and, moreover, samples were exchanged into the SEM by means of a device which maintained an Ar overpressure during the transfer process. Although samples which were rapidly exchanged into a microscope without using the transfer device did not give any obvious indication of macroscopic reactivity, it was found that even brief air exposure of $NaAlH_4$ significantly altered the morphology of the material. By comparing Fig. 1a and b, one can see that the room air exposure resulted in the formation of deep cracks on the initially smooth, crystalline particles.

Two other factors required special consideration in these analyses. First of all, these materials have low electrical conductivity and were thus susceptible to charging under the electron beam used in an SEM. Thin conducting coatings were evaluated, but were found to alter the surface appearance and, furthermore, difficulty was experienced in preventing air exposure during the added steps needed to coat samples. It was determined that adequate surface detail could be resolved simply by imaging at a low voltage (2 kV) in a field-emission SEM (JEOL 6400F). This imaging condition generally produced some horizontal streaking in images due to charging. However, as can be seen in the figures, the streaking artifact does not prevent the observation of particle size, shape and surface morphology.

The second factor was the susceptibility of these materials to electron beam damage. An example of modest beam damage can be seen by comparing Fig. 1a and c. The two images are of the same particle, but the image in Fig. 1c was recorded after the particle was examined for some time. The change in surface appearance is readily discernible. Also, observations of the relative Na to Al peak heights during acquisition of EDS data indicated that some Na content was being lost from the surface or near-surface region of particles during beam exposure. In order to minimize this surface damage, beam currents were kept as low as practical while maintaining adequate signal-to-noise ratio in the images. Focus and tune-up were typically made on areas adjacent to where images were recorded and EDS analyses were made.

Elemental composition within the near-surface region of particles was determined by EDS analyses using a 6 kV electron beam. This beam energy yielded adequate count rates for the excitation energies of interest (which minimized the time needed to acquire spectra) without excessive charging effects and damage production. Monte Carlo simulations using SANDYL [5] yielded an electron penetration depth of about 0.5 μm for 6 keV electrons in the

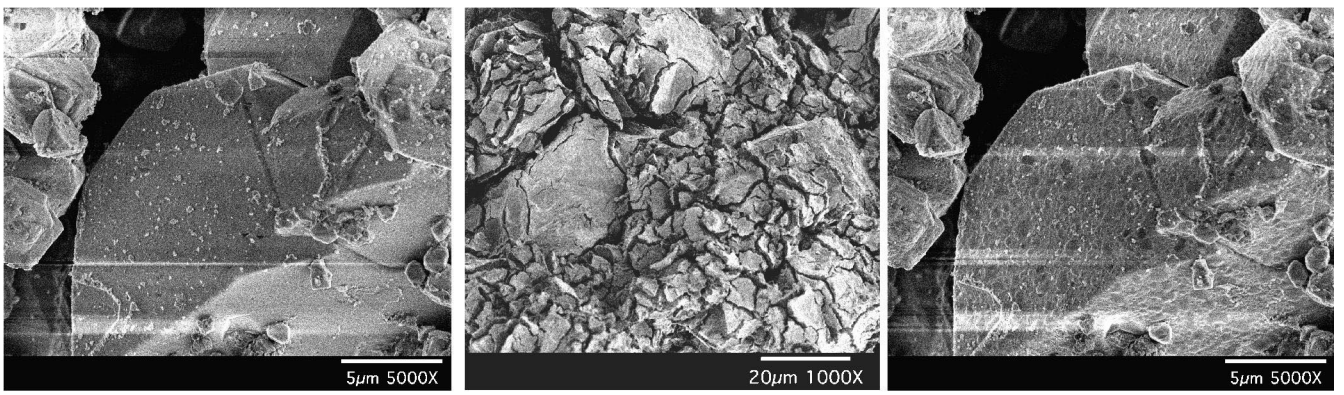

Fig. 1. Scanning electron micrographs showing the effects of air exposure and electron beam damage. (a) Image of $NaAlH_4$ as purified and prior to the catalyst doping process. (b) Image of $NaAlH_4$ after brief air exposure showing deep cracks due to reaction with oxygen and water vapor. (c) Image of the same region as in (a) after excessive beam exposure. Surface features are a product of electron beam damage.

alanate. Excitation energies for the K lines of Na and Al are of the order of 1 keV, so the sampling depth of the elemental analysis is somewhat less than the total range. As seen in Fig. 1, many of the particles in the starting material were much larger than a few micrometers and, hence, this technique gives an indication of the relative elemental content of the surface and near-surface region. Some spectra were also acquired at a beam energy of 10 kV and, as expected, these yielded results closer to bulk elemental concentrations. Measurements were made under a number of spatial beam conditions — large area scans to determine average values, small area scans at high magnification for individual particles or regions of particles, and spot mode, where a focussed beam was fixed at a given point to examine correlations of surface feature or morphology with elemental content.

One last issue to be recognized is that desorption has been found to occur, albeit slowly, in catalyst-doped tetrahydride at room temperature. Since there is some delay between material preparation and SEM observations, the conversion of some of the surface to the hexahydride, Na_3AlH_6, may have occurred. No attempt was made to examine rehydrided material after cycling.

2.2. Material preparation

In addition to examining the effects of desorption and absorption cycling, the effects of mechanical milling were also considered. A liquid alkoxide process developed by Jensen et al. [2] was employed to add catalyst to the alanate. In this process, alanate powders, purified by solvating in THF, decanting and vacuum drying, were mixed with a combination of 2 mol% $Ti(OBu^n)_4$ and 2 mol% $Zr(OPr)_4$ and homogenized by mechanically milling the mixture in a ball mill (SPEX® mill). The resultant particle sizes and morphology were examined following a brief ball milling (1–2 min) and also after a long, 3 h ball milling.

Samples for the intermediate and final phases (Eqs. (1) and (2)) were prepared from the doped starting material using quantitative hydrogen desorption measurements and verified by XRD observations. The intermediate hexahydride material was only examined during the first desorption cycle.

3. Results

The particle size and morphology resulting from the alkoxide doping process can be seen in Fig. 2a–c. Fig. 2a and b show the doped material after a short (1–2 min) ball milling used simply to mix and homogenize the mixture. A relatively thick surface coating is evident by comparing Fig. 2a with Fig. 1a. The well-defined angular features of the individual particles are now much smoother. Although the particle size has not changed, there is some indication of clustered particles which have agglomerated during the doping procedure. Prior to adding the catalyst, the $NaAlH_4$ particles were roughly equiaxed and ranged in size from about 2 μm to over 20 μm. After doping, some larger particles were observed, presumably formed by agglomeration of the initial material. Following 3 h of ball milling, the material has a greater range of sizes, as seen in Fig. 2c. Some of the larger particles in the figure are over 150 μm long, while particles as small as 2 μm are also present. One might intuitively expect that the longer ball milling would result in the breakup of particles and a generally smaller average particle size. However, our observations suggest that with the liquid catalyst, longer ball milling simply results in more agglomeration of material and no significant breakup into smaller particles of $NaAlH_4$.

EDS measurements on the as-prepared alkoxide-doped material showed much larger oxygen concentrations com-

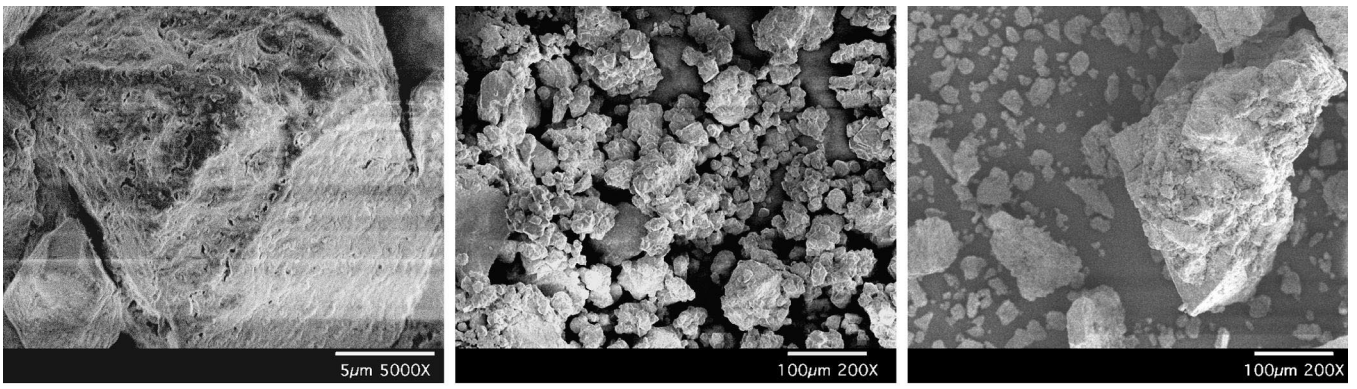

Fig. 2. Scanning electron micrographs of $NaAlH_4$ after Ti/Zr catalyst added using a wet alkoxide precursor and mechanical milling. (a) Image of material at same magnification as Fig. 1a, showing the residue of the liquid alkoxide coating the surface. (b) Lower magnification image showing the particle sizes after a short mechanical milling time (1–2 min). (c) Particle size range after 3 h of mechanical milling showing some agglomeration of particles into larger clusters.

pared with the undoped material. The surface oxygen concentration for the alkoxide-doped material, inserted into the SEM using a sample exchange mechanism to prevent air exposure, was measured under a number of different scanning conditions and on many different particles. The average value was found to be approximately 60 at.% oxygen. In contrast, measurements on undoped $NaAlH_4$ generally yielded a concentration of 5–7 at.% oxygen, an order of magnitude lower. These oxygen values are plotted in Fig. 3, along with the Na and Al concentrations, for all of the stages within the first desorption cycle. As mentioned earlier, since the initial state of the material is fully hydrided, the first cycle consists only of a desorption step and we consider the first gas phase absorption to be a part of the second absorption/desorption cycle. The data show some important features. The large concentration of surface oxygen introduced by the doping procedure is clearly evident and, furthermore, the oxygen is not removed during the elevated temperature (150°C) hydrogen desorption process. It should be mentioned that two other samples were found to retain oxygen concentrations in the range of 35–40 at.% even after five cycles at temperatures up to and exceeding 180°C during hydrogen absorption. The tenacity of the film introduced by the alkoxide process is also evident by the gas-stream impurities reported by Sandrock et al. [6] during repeated desorption and absorption cycles.

The desorption process and absorption/desorption cycles were found to significantly alter the morphology of the particles. Fig. 4a and b show electron micrographs taken during the first desorption cycle. These materials were initially prepared with a short mechanical milling time so that Fig. 1a can be considered to be a representative example of the starting material. Note, first of all, that there is more surface deformation associated with the reaction in Eq. (2), from the hexahydride to monohydride material (Fig. 4a vs. 4b), than from the tetrahydride to hexahydride reaction (Fig. 1a vs. 4a) described in Eq. (1). Furthermore, these images, as well as others at higher and lower magnifications, suggest that the individual particles accommodate the deformation without significant particle breakup. The lack of particle breakup was also observed in material which had been subjected to up to five absorption/desorption cycles. This behavior is in marked contrast to intermetallic hydrides, where particle breakup and fragmentation is an important part of the initial activation process for such materials.

Mapping of elemental composition using EDS was attempted in these first cycle dehydrided samples. Some variations in Na and Al concentrations were observed between different regions of individual particles and between different particles; however, no consistent trend was observed and no correlation could be made between elemental composition and identifiable surface features. In contrast, samples cycled five times did show compositional segregation.

The fully desorbed state after five cycles is shown in Fig. 5 for a single ‘particle’. The deformation has now developed into two distinct features — smooth nodules and porous surfaces. Examples of both features are identified in the micrograph. There are also deep pores extending well into the particle. The nodules are typically of the order of 1 μm across, while the somewhat larger porous regions are generally adjacent to groups of nodules. Interestingly, differences in elemental composition were found between the two features. The smooth nodules were determined to be consistently Na-rich, with an average Al/Na ratio of 0.7. Furthermore, the nodules did not have detectable

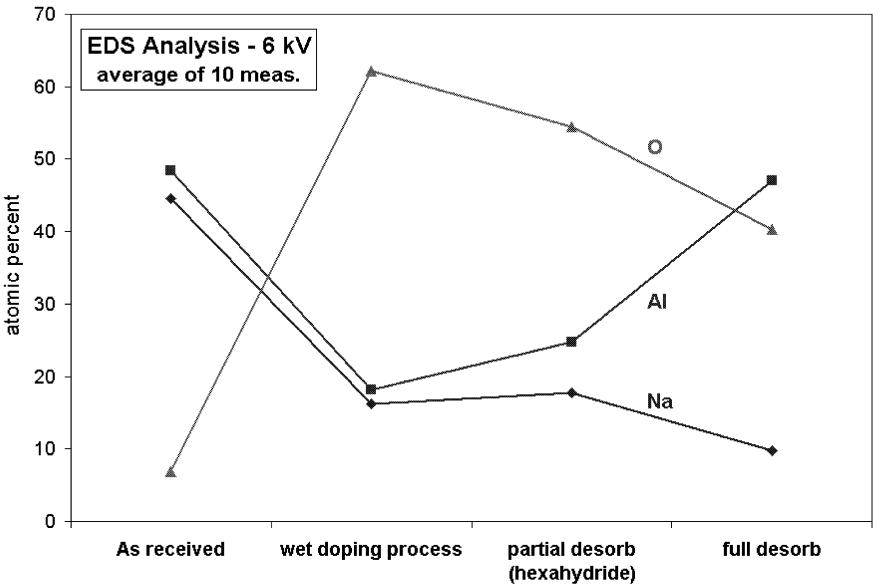

Fig. 3. Plot of elemental compositions determined by EDS analysis on material during the processing and the first desorption cycle.

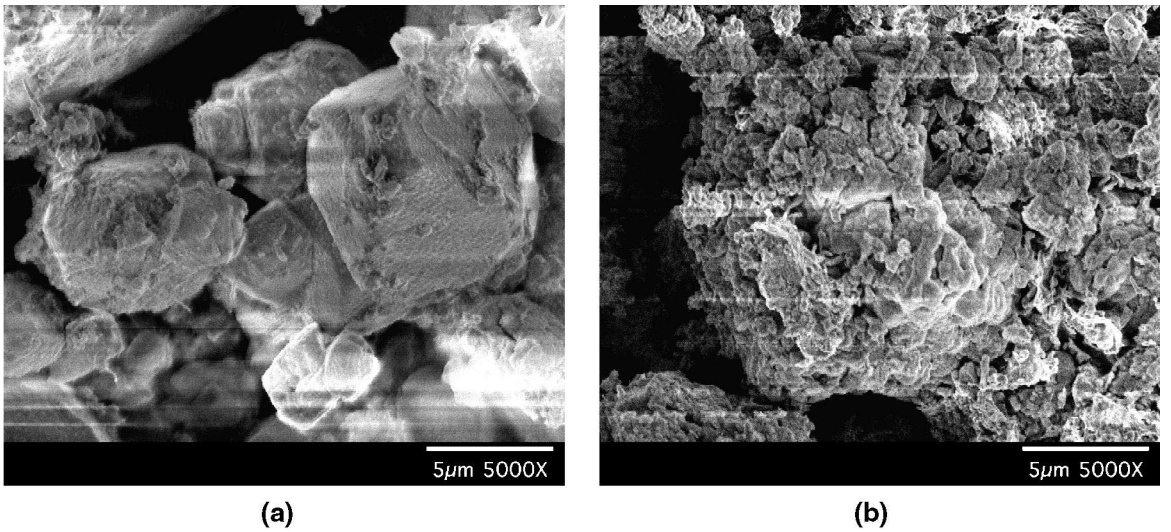

Fig. 4. Scanning electron micrographs of material during the first desorption cycle. (a) Na_3AlH_6 and Al remaining after hydrogen desorption from $NaAlH_4$. (b) Material after complete desorption to NaH and Al phase.

levels of Ti catalyst. Surface regions which exhibited a porous microstructure, on the other hand, were always Al-rich with an average Al/Na ratio of 2. These regions were also found to have catalyst concentrations equivalent to the starting material.

4. Summary and conclusions

1. The alkoxide process used to dope $NaAlH_4$ with a Ti–Zr catalyst resulted in the formation of an oxygen-rich coating which was relatively stable. Absorption and desorption cycles at elevated temperatures reduced some of the oxygen content, but did not eliminate the residue. This is consistent with the results of Sandrock et al. [6] which showed continued release of hydrocarbon species in the hydrogen stream during repeated desorption cycles.
2. Mechanical ball milling, used to mix the alanate and liquid catalyst precursor, did not break up particles, but rather caused some agglomeration into larger clusters of particles. Use of such a mechanical technique to produce smaller particles, which may be desirable to improve kinetic properties of hydrogen release and absorption, may be successful with another dry or liquid catalyst precursor.
3. Significant changes in particle morphology were observed within the first desorption steps and were further developed with repeated absorption/desorption cycling. Fracture and fragmentation of particles was found to be far less than typically seen during hydrogen cycling of intermetallic hydrides.
4. The elemental segregation of Na and Al found in particles after multiple absorption/desorption cycles may be a factor in the relatively low absorption capacity reported by Sandrock et al. [6] for Na alanate doped by the same technique. That is, the physical separation between the required materials may hinder the formation of the ionic compounds. Furthermore, the correlation observed between the Ti catalyst and Al-rich surfaces, and the lack of Ti in the Na-rich nodules, may not only play a role in reducing the ability to reconstitute the compounds, but also suggests that the Ti catalyst may be chemically associated with Al from the alanate.

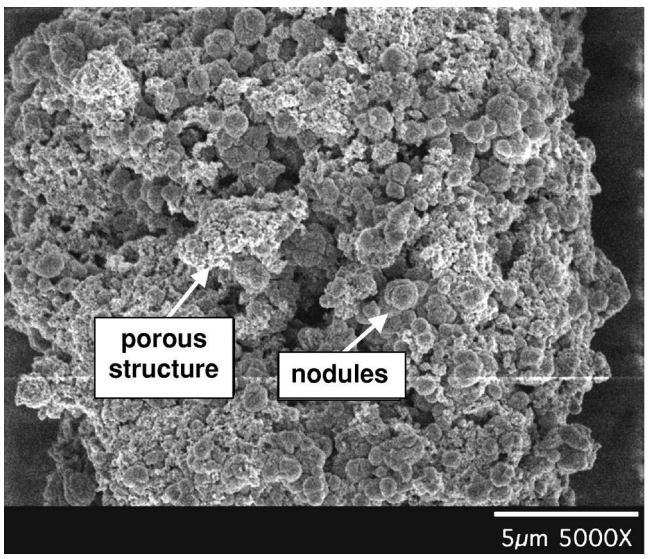

Fig. 5. Scanning electron micrograph of fully desorbed material after five absorption/desorption cycles.

Acknowledgements

Funding is provided by the U.S. Department of Energy, Office of Power Technologies, Hydrogen Program Office under contract No. DE-AC36-83CH10093. We wish to thank Don Meeker for his expert technical assistance and Jeff Chames for assistance in the electron microscopy and X-ray analysis. Special thanks are due Dr. Satoshi Takara for his sample preparation efforts and to Dr Gary Sandrock for many helpful discussions. The SANDYL calculations were performed by Dr. Arlyn Antolak.

References

[1] B. Bogdanovic, M. Schwickardi, J. Alloys Comp. 253 (1997) 1; B. Bogdanovic, R.A. Brand, A. Marjanovic, M. Schwickardi, J. Tolle, J. Alloys Comp. 302 (2000) 36.

[2] C.M. Jensen, R.A. Zidan, N. Mariels, A.G. Hee, C. Hagen, Int. J. Hydrogen Energy 24 (1999) 461; R.A. Zidan, S. Takara, A.G. Hee, C.M. Jensen, J. Alloys Comp. 285 (1999) 119.

[3] K.J. Gross, S.E. Guthrie, S. Takara, G.J. Thomas, J. Alloys Comp. 297 (2000) 270.

[4] A. Zaluska, L. Zaluski, J.O. Strom-Olsen, J. Alloys Comp. 298 (2000) 125.

[5] H.M. Colbert, Sandia National Laboratories Report, SCL-DR-720109, March 1973.

[6] G. Sandrock, K. Gross, G. Thomas, C. Jensen, D. Meeker, S. Takara, J. Alloys Comp. 330–332 (2002) 696.